Chemical Accuracy Obtained in an Ab Initio Molecular Dynamics Simulation of a Fluid by Inclusion of a Three-Body Potential

Barbara Kirchner, Elena Ermakova, Jan Solca, and Hanspeter Huber*

Abstract: A three-body potential was included in a molecular dynamics simulation program to calculate structural and thermodynamic properties of liquid and liquid-like states of neon. In general the agreement with the experiment is within 1%. For high densities at 300 K the pressure shows three-body effects up to 3%. Accounting for these effects with the new three-body potential allows one to predict the pressure at high densities not easily accessible to experiment. At very low temperatures translational quantum effects, which are not treated adequately in the present simulations, are sizeable.

Keywords: molecular dynamics · neon · supercritical fluids · thermodynamics · three-body interactions

Introduction

As much interesting chemistry takes place in the liquid phase, one goal of theoretical chemists has been to achieve a more accurate description of liquid systems. Preferably, in order to provide close correspondence with experiment, one would like deviations between calculated and experimental properties to be less than 1%. In order to reach this accuracy within the constraints imposed by present computational facilities we need to systematically determine the macroscopic consequences of various microscopic changes.

In the theory of fluids, computer simulations of noble gases as test systems have provided valuable insights relevant to more complex systems. Recent advances in liquid noble gas molecular dynamics and Monte Carlo simulations have focused on three key areas: the use of the best pair potential, the inclusion of quantum corrections and the accommodation of many-body effects.

Initial efforts involved replacement of simple model potentials, in particular the Lennard-Jones potential, with more precise pair potentials (see for example the Ar potential of Woon[1]), which have been applied in molecular dynamics simulations.[2] A systematic study of the influence of basis-set size on ab initio potentials and simulated properties has been undertaken for neon. A first potential NE1[3] was constructed based on ab initio total energy calculations with a basis set consisting of 71 primitive Gaussians contracted to 45 functions per atom, and a second one NE2[4] with 112 primitives contracted to 84 functions, both including correlation by MP4(SDTQ) perturbation theory. The improvement of the pair potential was found to have a large effect on pressure and energies, particularly at high densities, a lesser but still significant influence on derived thermodynamic properties like molar heats, compressibilities, etc., but hardly any effect on structure and transport properties.[4, 5]

The second question to be investigated is the importance of quantum corrections for liquid noble gases. This is explored in semiclassical simulations by Ermakova et al.,[6] who showed that virtually exact pair distribution functions are obtained by including a quantum effective Wigner–Kirkwood potential.

The last important correction should come from the inclusion of many-body effects. A short discussion of its relevance is given in the preceding paper[7] and more details are found in recent reviews.[8, 9] In this publication we investigate the importance of three-body effects on fluid neon by combining the non-pair-additive part of the three-body potential (see preceding paper) with two different pair potentials. We also investigate which properties are sensitive to three-body interactions (TBI) and when the latter are negligible.

Computational Methods

The potential energy in the absence of an external field is given in Equation (1) where $\mathbf{r}_i$ is the vector pointing to atom i, the first summation is over the pair potentials ΔE_2 (two-body terms), the second over the non-pair-additive parts of the three-body potential $\Delta\Delta E_3$ (three-body terms, hereafter referred to as non-additive TBI) and so on. In this work only two- and three-body terms are included.

[*] Prof. Dr. H. Huber, B. Kirchner, J. Solca, E. Ermakova[+]
Institut für Physikalische Chemie der Universität Basel
Klingelbergstrasse 80, CH-4056 Basel (Switzerland)
Fax: (+41) 61-267-3855
E-mail: huber@ubaclu.unibas.ch

[+] Kazan State University (Russia)

  0947-6539/98/0403-0383 $ 17.50+.25/0

$$E_{\mathrm{pot}} = \sum_i \sum_{j>i} \Delta E_2(\mathbf{r}_i,\mathbf{r}_j) + \sum_i \sum_{j>i} \sum_{k>j} \Delta\Delta E_3(\mathbf{r}_i,\mathbf{r}_j,\mathbf{r}_k) + \sum_i \sum_{j>i} \sum_{k>j} \sum_{l>k} \Delta\Delta E_4(\mathbf{r}_i,\mathbf{r}_j,\mathbf{r}_k,\mathbf{r}_l) + \ldots \quad (1)$$

The three-body potential obtained in the preceding paper was built into a molecular dynamics program for simulations in the microcanonical (NVE) ensemble, which employs the Verlet leap-frog algorithm for a cubic box with periodic boundary conditions. More details about the original program and the parameters applied in the simulations can be found in ref. [10]. To include the three-body terms changes in the program are mainly necessary in the force routine in which not only forces, but also energies and the virial coefficient are calculated. The conventional double loop over the particles is nested with an additional third loop. In the double loop the two-body terms are calculated as before and in the third embedded loop the three-body terms are added. By using this scheme we are able to take advantage of the fact that the non-additive TBI can be combined with different pair potentials.

We have recalculated the thermodynamic properties determined by Eggenberger et al.[5] within the pair potential approximation, this time including three-body effects. The following definitions have been used [Eqs. (2), (3) and (4)].

$$U = \langle E \rangle = \langle E_{\mathrm{pot}} + E_{\mathrm{kin}} \rangle \quad (2)$$

$$E_{\mathrm{pot}} \approx \sum_i \sum_{j>i} \sum_{k>j} \Delta E_3 \approx \sum_i \sum_{j>i} \Delta E_2(\boldsymbol{r}_{ij}) + \sum_i \sum_{j>i} \sum_{k>j} \Delta\Delta E_3(\boldsymbol{r}_{ij},\boldsymbol{r}_{ik},\boldsymbol{r}_{jk}) + E_{\mathrm{LRC},2} + E_{\mathrm{LRC},3} \quad (3)$$

$$E_{\mathrm{kin}} = {}^3/_2 RT = {}^1/_2 \sum_i m_i v_i^2 \quad (4)$$

The potential energy E_{pot} consists of sums over the pair potential ΔE_2 and the nonadditive TBI $\Delta\Delta E_3$, which are both given in terms of interatomic distances, and the corresponding long-range corrections E_{LRC} (see below). R is the universal gas constant, T the temperature and m_i and v_i are the mass and the velocity of particle i, respectively. Sums are taken over N particles; $\langle \ldots \rangle$ is the time average. The pressure P [Eq. (5)]consists of the ideal gas pressure and terms taking care of the intermolecular interactions through the pair virial W_2 and non-additive part of the three-body virial W_3 [Eq. (6)], and the corresponding long-range corrections.

$$P = \rho(RT + W_2 + W_3) + P_{\mathrm{LRC},2} + P_{\mathrm{LRC},3} \quad (5)$$

$$W_3 = \sum_i \sum_{j>i} \sum_{k>j} (\boldsymbol{r}_{ij} \nabla_{r_{ij}} (\Delta\Delta E_3) + \boldsymbol{r}_{ik} \nabla_{r_{ik}} (\Delta\Delta E_3) + \boldsymbol{r}_{jk} \nabla_{r_{jk}} (\Delta\Delta E_3)) \quad (6)$$

The molar heat capacity $C_{\mathrm{V,m}}$ [Eq. (7)] at constant volume contains the fluctuation of the kinetic energy. Three-body interactions affect this equation only indirectly, through the different dynamics of the particles in the system. For the calculation of the thermal pressure coefficient γ_{V} [Eq. (8)], the fluctuation of the temperature $\langle \delta T^2 \rangle$ and time averages of

$$C_{\mathrm{V,m}} = {}^3/_2 R \{1 - {}^2/_3 N (R\langle T \rangle)^{-2} \langle \delta E_{\mathrm{kin}}^2 \rangle\}^{-1} \quad (7)$$

$$\gamma_{\mathrm{V}} = C_{\mathrm{V,m}} \rho [{}^2/_3 - N(R\langle T^2 \rangle)^{-1} (R\langle \delta T^2 \rangle + \langle TW \rangle - \langle T \rangle \langle W \rangle)] \quad (8)$$

the virial W (the sum of W_2 and W_3) are needed. The virial contains the nonadditive TBI. The adiabatic compressibility β_{S} [Eq. (9)] includes the fluctuation of the pressure, and the hypervirial χ. For simplicity, and to save computing time, the hypervirial (defined in ref. [11]) was treated only for the pair potential. This is not exact; however the contribution would have been small. The isothermal compressibility β_{T} [Eq. (10)] contains the

$$(\beta_{\mathrm{S}})^{-1} = -\langle \delta P^2 \rangle (R\rho\langle T \rangle)^{-1} N + {}^2/_3 R\rho\langle T \rangle + \langle P \rangle + \rho\langle \chi \rangle \quad (9)$$

$$(\beta_{\mathrm{T}})^{-1} = (\beta_{\mathrm{S}})^{-1} - \langle T \rangle \gamma_{\mathrm{V}}^2 (\rho C_{\mathrm{V,m}})^{-1} \quad (10)$$

hypervirial through the adiabatic compressibility β_{S}, hence it is also not corrected exactly. This latter statement is also true for all the following properties: $C_{\mathrm{P,m}}$ the molar heat capacity at constant pressure [Eq. (11)], c the speed of sound [Eq. (12)] and μ the differential Joule–Thompson coefficient [Eq. (13)].

$$C_{\mathrm{P,m}} = C_{\mathrm{V,m}} \beta_{\mathrm{T}} / \beta_{\mathrm{S}} \quad (11)$$

$$c = (\rho\beta_{\mathrm{S}})^{-1/2} \quad (12)$$

$$\mu = (\beta_{\mathrm{T}} \gamma_{\mathrm{V}} \langle T \rangle - 1)/(\rho C_{\mathrm{V,m}}) \quad (13)$$

Use of a Verlet neighbour list, and truncation of both the pair potential and the nonadditive part of the three-body potential, leads to three important radii. The list radius r_{list} is chosen to be 3.1 σ, σ being 283.8 pm for NE 1 and 279.2 pm for NE 2. For the two-body and three-body terms of the potential the cutoff radii were set at $r_{\mathrm{cut2}} = 2.7\,\sigma$ and $r_{\mathrm{cut3}} = 1.34\,\sigma$, respectively. r_{cut3} has to be smaller than half of r_{cut2}, as a result of the way we have implemented the loops and the long-range corrections. A nonadditive $\Delta\Delta E_3$ contribution is included in the third loop if all distances are within r_{cut2} and at least two of them within r_{cut3}. Similarly, within the third loop a subroutine is called that calculates the pressure $P_3 = \rho \times W_3$ due to the three-body interactions.

The truncation of the potentials requires a correction. Long-range corrections $E_{\mathrm{LRC},2}$ and $P_{\mathrm{LRC},2}$ for the pair potential are described in detail in ref. [11]. We also have to add long-range corrections for the truncation of the nonadditive part of the three-body potential. The energy correction is given by Equation (14).[12]

$$E_{\mathrm{LRC},3} = {}^1/_6 N_{\mathrm{A}}^2 \rho^3 \iiint g(\mathbf{r}_1,\mathbf{r}_2,\mathbf{r}_3) \Delta\Delta E_3 \, d\boldsymbol{r}_1 d\boldsymbol{r}_2 d\boldsymbol{r}_3 \quad (14)$$

N_{A} is Avogadro's constant, ρ the particle density, and $g(\mathbf{r}_1,\mathbf{r}_2,\mathbf{r}_3)$ the trimer distribution function. The integration is performed over the space complementary to the one accounted for in the loop. Applying the Kirkwood superposition approximation, $g(\mathbf{r}_1,\mathbf{r}_2,\mathbf{r}_3)$ can be replaced by the product of the three pair distribution functions $g(r_{12})g(r_{13})g(r_{23})$ and the integration variables transformed to the interatomic distances r_{12}, r_{13}, and r_{23}, by the relation shown in Equation (15);[13] thus Equation (14) turns into Equation (16). For practical reasons we use two interatomic distances and the angle between them as variables together with the Jacobian $r_{12} r_{13} \sin\Theta / r_{23}$ for the long-range energy correction [Eq. (17)].

$$d\boldsymbol{r}_1 d\boldsymbol{r}_2 d\boldsymbol{r}_3 = 8\pi^2/\rho \times r_{12} r_{13} r_{23} dr_{12} dr_{13} dr_{23} \quad (15)$$

$$E_{\mathrm{LRC},3} = {}^4/_3 \pi^2 N_{\mathrm{A}}^2 \rho^2 \iiint g(r_{12}) g(r_{13}) g(r_{23}) \Delta\Delta E_3 \, r_{12} r_{13} r_{23} dr_{12} dr_{13} dr_{23} \quad (16)$$

$$E_{\mathrm{LRC},3} = {}^4/_3 \pi^2 N_{\mathrm{A}}^2 \rho^2 \iiint g(r_{12}) g(r_{13}) g(r_{23}) \Delta\Delta E_3(r_{12},r_{13},\Theta) r_{12}^2 r_{13}^2 \sin\Theta \, dr_{12} dr_{13} d\Theta \quad (17)$$

The integration limits were chosen to include only those trimers which are not treated in the force routine. The limits for the first two integrations are r_{cut3} and infinity, for the last integration zero and π. Note again that r_{cut3}

Abstract in German: *Zur Berechnung von Struktur und thermodynamischen Eigenschaften von flüssigem und superkritischem Neon wurde ein Drei-Teilchen-Potential in ein Moleküldynamik-Programm integriert. Die berechneten Eigenschaften stimmen mit einer Abweichung innerhalb von ca. 1 % mit den experimentellen überein. Für hohe Dichten zeigt der Druck bei 300 K einen Drei-Teilchen-Anteil von bis zu 3 %. Durch Berücksichtigung dieses Anteils im neuen Drei-Teilchen-Potential können Drücke bei hohen Dichten vorausgesagt werden, die dem Experiment kaum zugänglich sind. Die Quantelung der Translationsbewegung der Atome bei sehr tiefen Temperaturen wird in den vorliegenden Simulationen nicht berücksichtigt.*

  0947-6539/98/0403-0384 $ 17.50+.50/0 *Chem. Eur. J.* **1998**, *4*, No. 3

should be less than half of r_{cut2}, otherwise some cases will be handled neither in the force loop nor in the TBI long-range subroutine. The integration is performed numerically by a three-dimensional Gaussian quadrature.[14] The corresponding correction for the pressure is given in Equation (18). The three-body long-range corrections are added at the end of the calculations, when the pair distribution function is available from the simulation.

$$P_{LRC,3} = -{}^{4}/_{9}\pi^2 N_A^2 \rho^3 \int\int\int g(r_{12})g(r_{13})g(r_{23})\; P_3(r_{12},r_{13},\Theta) r_{12}^2 r_{13}^2 \sin\Theta dr_{12} dr_{13} d\Theta \quad (18)$$

Results and Discussion

In the following we refer to the older potential given by Eggenberger et al.[3] as NE1 and the newer one as NE2.[4] NE1/TBI is the older potential including the three-body interaction as calculated in the preceding paper, whereas NE2/TBI is the newer pair potential NE2 combined with the nonadditive three-body interaction calculated with the smaller basis set NE1 in the preceding paper. This latter approach may be questioned. It has been pointed out in the literature,[15] however, that the nonadditive part of the three-body interaction shows much faster convergence with the basis set size than the pair interaction.

Before discussing the present results in detail, let us consider an interpretation of the deviations from experiments in our previous simulations. Simulations with the pair potential NE2 yielded very accurate properties at low pressures (note that in this paper a pressure of 100 MPa = 1000 bar is called a low pressure, as it is at the lower end of the pressures investigated; this should not be confused with a gas at low pressure). For example, in the supercritical state at 300 K and 100 MPa the pressure calculated with the pair potential NE2 is 1.8 MPa too large (4.3 MPa for NE1). However, at greater pressures the deviations increase, reaching 39 MPa at 1000 MPa (98 MPa for NE1). These results do not suggest that the dispersive interactions need an improvement, but rather that the repulsive part of the potential might not be fully adequate. The two pair potentials NE1 and NE2 are very similar in the long-range part. One main improvement of NE2 is the depth of the potential near and at the equilibrium distance (108.4 μE_h for NE1 and 120.6 μE_h for NE2; the experimental depth is estimated to be 130.6 ± 4.6 μE_h). The well depth together with other pair properties (for a more detailed discussion see ref. [4]) gives us an estimate of the difference between NE2 and the true pair potential that is slightly smaller than the difference between NE1 and NE2. We will refer to this in the discussion below. A second important change is the shift of the repulsive wall to smaller distances (Figure 1). At high pressures this will be more important and we can try to give a qualitative interpretation in terms of a hard-sphere model.

For a hard-sphere model the Percus–Yevick equations can be solved analytically[16] and the pressure given as a function of density. It can be shown that the difference in pressure between systems of smaller and larger spheres is small at low density; however, the deviation increases sharply as the density is raised. This behaviour parallels that observed in our MD simulations, that is, increased deviation between calculated and experimental pressure as the density is raised, and

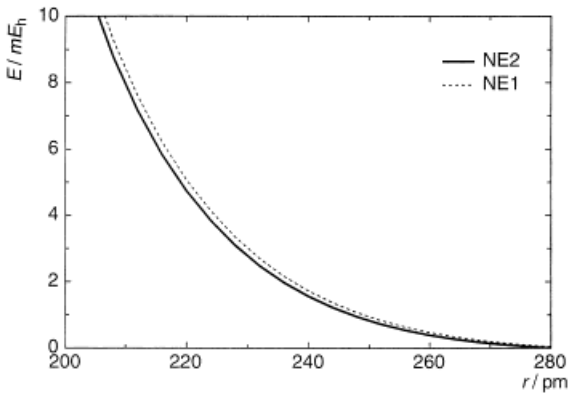

Figure 1. The repulsive part of the ab initio potentials NE1 and NE2 applied in the simulations.

significantly greater deviation for NE1 than for NE2 (see Figure 3). We can consider the NE1 model atoms as larger spheres and the NE2 model atoms as smaller spheres, as a result of the shift in the repulsive wall described above. Note that estimated experimental diameters correspond to yet smaller spheres. The hard-sphere results indicate that the improvement in calculated pressure from NE1 to NE2 can be attributed almost entirely to the improvement in the repulsive part of the potential. For the three body interactions to result in further improvement, they would need to modify the short-range repulsive part of the potential, rather than the long-range behaviour. Inclusion of Axilrod–Teller interactions, for example, is unlikely to produce an improvement in this case. Figure 3 of the preceding paper shows for an isosceles triangle that $\Delta\Delta E_3$ is indeed very negative at a distance σ, thus leading on average to smaller spheres, which in turn will reduce the pressure, as we will see. At very short distances it becomes positive again, but this has no influence at the temperatures studied. The long-range part of the nonadditive TBI is negligible compared with the repulsive part. It should be pointed out that this might be a result of the limited order of perturbation we used in our correlation calculations; however, in view of the excellent agreement of all bulk properties calculated at low pressure, there is no reason to assume that a more accurate attractive part should play a significant role.

In summary, the previous deviations of simulated from experimental results were a result of defects in the repulsive part of the potential, rather than in the attractive part. We will now discuss the present results and give more detailed arguments.

Structure: For a discussion of the structure we use the radial distribution function g. It has been shown previously[6] that the improvement of the potential from NE1 to NE2 has very little influence on g. At temperatures of 26 and 36 K the first maximum was identical within statistical error, while at 42 K it increased by 3% from NE1 to NE2. It was estimated[4] that the deviation of NE2 from the experimental pair potential is smaller than the deviation of NE1 from NE2. Hence, an improvement of the potential should produce no significant change in g. Furthermore, Ermakova et al.[6] were able to show by means of a quantum effective potential that the quantum-corrected g functions are virtually identical with the

experimental functions. Hence, we did not expect much change due to the three-body interaction. This was indeed the case and in a graph of the g function one can hardly see any change. However, if we take a close look at the first peak of the g function as given in Figure 2, we see a small shift of

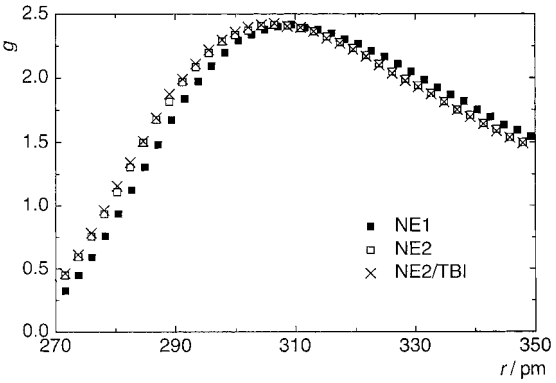

Figure 2. An enlarged portion of the g pair distribution function at 36 K showing the shift of the first peak to smaller distances with improved levels of calculation.

about 2 – 3 pm towards smaller radii between NE1 and NE2, and an even smaller shift of about 0.5 pm in the same direction, if we include the three-body interaction. A similar small shift is observed in the supercritical state at 298 K and 1000 MPa. This is in agreement with the preceding discussion about the potentials shown in Figure 1.

We conclude that for rare gases quantum effects at low temperatures are important, whereas three-body effects and the quality of the pair potential are of minor importance. If this could be generalised for the structure of molecular liquids it would be of great help for the calculation of accurate solvent effects as performed by several authors for infrared absorption,[17] nuclear quadrupole couplings,[18–22] and NMR shifts.[23, 24]

Pressure: As mentioned above and shown in Table 1 and Figure 3,[25] the pressure simulated with pair potentials deviates increasingly from experimental values at higher densities. If we think in terms of hard spheres with too large

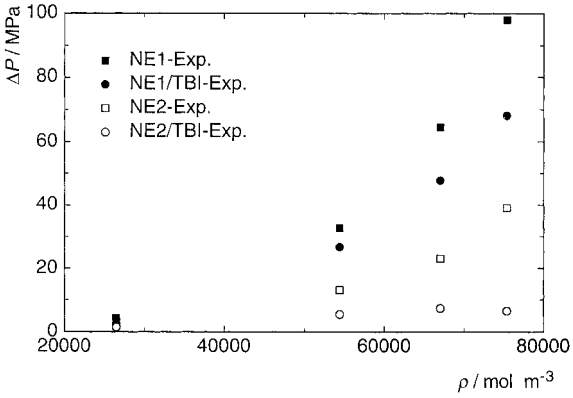

Figure 3. Deviations between calculated and experimental pressure versus the density at a temperature of 298 K. The points correspond to pressures of 100, 400, 700 and 1000 MPa, respectively.

radii, we expect such deviations as those found in all our previous simulations. The smaller spheres of NE2 improve the results more than the inclusion of three-body interactions in simulations with NE1. This could be an indication that many deviations from experiment attributed in the literature to many-body effects could be the result of inadequate pair potentials. However, there is also an improvement due to the inclusion of the three-body interaction, although it has only about half the size of the improvement between NE1 and NE2. Comparison of the improvements of the pressure in Figure 3 when three-body interactions are included with NE1 or NE2 shows that they are nearly additive.

At a first glance Figure 3 gives the impression that the present calculations on the NE2/TBI level are virtually exact. However, we must be aware that a better pair potential could yield smaller pressures which deviate slightly more (with a negative sign) from experiment than the present results. Nevertheless, the results will be within typical chemical accuracy and we have shown here that three-body interactions are quite small, yielding a contribution of only about 3 % even at a pressure of 1000 MPa. The situation could be different for molecular liquids at ambient temperatures, as in those cases the attractive part of the potential might play a more important role.

Table 1. Energy U and pressure P[a] calculated on different levels and compared with the experimental values U_{exp} and P_{exp}.

T (K)	ρ (mol m^{-3})	P_{NE1} (MPa)	$P_{NE1/TBI}$ (MPa)	P_{NE2} (MPa)	$P_{NE2/TBI}$ (MPa)	P_{exp} (MPa)	U_{NE1} (J mol^{-1})	$U_{NE1/TBI}$ (J mol^{-1})	U_{NE2} (J mol^{-1})	$U_{NE2/TBI}$ (J mol^{-1})	U_{exp}[b] (J mol^{-1})
298	26472	104.4	103.9	101.8	101.5	100	3477	3461	3433	3424	3372
298	54411	432.7	426.7	413.1	405.5	400	3575	3546	3456	3422	(3289)
298	66998	764.6	747.8	723.0	707.4	700	3944	3882	3746	3688	
298	75373	1098.0	1068.2	1039.1	1006.6	1000	4377	4283	4115	4025	
100	50864	118.3	114.8	107.0	103.5	100	331	309	255	234	
200	34650	108.0	106.8	103.8	102.8	100	2033	2025	1981	1977	
298	26472	104.4	103.9	101.8	101.5	100	3477	3461	3433	3424	3372
400	21527	103.6	103.3	101.8	101.4	100	4864	4860	4833	4830	4745
500	18178	102.6	102.6	101.4	101.2	100	6192	6189	6166	6163	
28	63532	37.4	29.5	17.1	9.3	20	– 1212	– 1249	– 1307	– 1343	

[a] The equilibrium temperatures of the simulations usually deviate slightly from the exact temperatures given in the table. As pressure and energy are very sensitive, the values from the simulations were interpolated to correspond exactly to the temperatures given in the first column. The errors caused by the interpolation, the statistics and the simulation parameters are estimated to be about 0.5 – 1 % for pressures and 0.5 % for energies. [b] Experimental values interpolated and extrapolated (in parentheses) from ref. [25].

0947-6539/98/0403-0386 $ 17.50+.50/0 *Chem. Eur. J.* **1998**, *4*, No. 3

Figure 4 shows the pressures at 100 MPa as a function of temperature. To understand the behaviour we should recognise the noticeable increase of the densities at lower temperatures, reaching a value not far from liquid densities at 100 K. At higher temperatures and, hence, low densities (i.e., on the

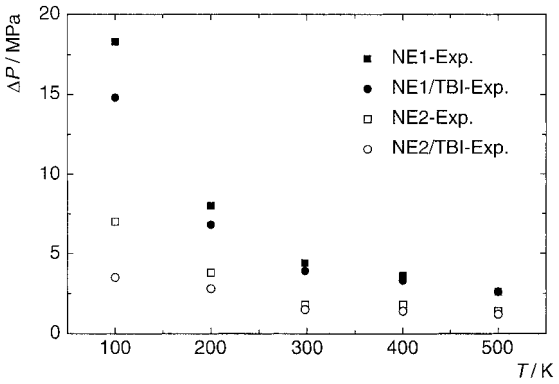

Figure 4. Deviations between calculated and experimental pressure versus the temperature at an experimental pressure of 100 MPa. The densities change from 18178 to 50864 mol m^{-3} (see Table 1).

right side of the graph) the three-body interaction contributes little. Therefore, the remaining error (although close to the technical error, see below) probably results from the pair potential. Indeed, the gap between NE2 and the experimental pressure is slightly smaller than between NE1 and NE2, as is the potential depth of the pair potential. This suggests that the remaining errors result from the inaccuracies of the pair potential NE2.

The statistical error of the simulated pressure is typically less than 0.2% with an additional error of about 0.1% that stems from the temperature correction. An error owing to the cutoff radii, the step size and the limited number of atoms is estimated from simulations at 1000 MPa to be about 0.5%, which results in an overall technical error of the simulated pressures of 0.5 to 1%.

The last line of Table 1 needs a further comment. It is a phase point in the liquid state at very low temperature. Hence, translational quantum effects will be extremely important. An estimate of its size by perturbation theory was given by Eggenberger et al.,[4] who obtained a pressure of 33.6 MPa as compared with 17.1 MPa without corrections for the same state point with NE2 with the inclusion of quantum corrections. If, similarly, a factor of two is applied to the new result, a reasonable pressure of about 20 MPa results.

The pressure is probably the property most sensitive to errors in the intermolecular interactions. Hence, the present results with a typical deviation of about 1% from experiment, at temperatures that are not too low, are very satisfying.

Internal energy: The internal energies are given in Table 1. There are only few experimental values available for comparison. The deviations are less than 2%, that is, chemical accuracy is roughly attained for energies as well. Going from NE1 to NE2 the energies are lowered by about 40 J mol^{-1} at low pressures and up to about 250 J mol^{-1} at 1000 MPa. A rough estimate of what is expected from the change in the potential can be given as follows: The first shell in liquid neon has roughly 10 atoms corresponding to 5 pair interactions. The NE2 potential is about 10 μE_h (25 J mol^{-1}) less than NE1 in the equilibrium region, suggesting a lowering of the energy of the order of $5 \times 25 = 125$ J mol^{-1} in agreement with the above numbers. A further lowering of the energies by a similar amount caused by a more accurate pair potential would improve the present energies and make them virtually exact, if three-body interactions are included. On inclusion of three-body interactions the change in energy is again only less than half of the change observed between the two pair potentials. The largest three-body interaction (at 1000 MPa) is only slightly more than 2%. A comparison of the columns U_{NE1} with U_{NE2} in Table 1 on the one hand and U_{NE2} with $U_{NE2/TBI}$ on the other shows that the three-particle interaction is smaller than the improvement in the two-particle interaction. This means that a further improvement in the pair potential would have a sizeable effect. An estimate, as carried out for the pressure, yields an overall technical error that is due to simulation parameters and so on of about 0.5% for the energy.

As for the pressure, a very accurate energy is only obtained with an excellent pair potential. To use a very accurate pair potential is more important than to include three-body interactions, although at very high pressures the latter gain significance.

Derived thermodynamic properties: As previously reported,[5, 26] derived thermodynamic properties such as the thermal pressure coefficient, the adiabatic and isothermal compressibility, the thermal expansion coefficient, the Joule–Thompson coefficient, the speed of sound, and the molar heats at constant volume and pressure have been calculated with reasonable accuracy. Therefore, we did not expect much improvement as a result of many-body interactions. This was confirmed in the present simulations, in which all values were the same as those obtained with NE2 within statistical errors. Hence, we will only discuss the various properties briefly without giving an additional table with the values. Because translational quantum effects have unknown influences on the liquid phase point with temperature 28 K, we exclude this point from the discussion.

Comparison with experimental values, where available, shows that whereas the adiabatic compressibility is accurate within 1 to 2%, the isothermal compressibility deviates by up to 5%. Although this deviation is more or less within statistical error, the calculated values are systematically too low. Regarding the change from NE1 to NE2 simulated values,[5] it is likely that an improved pair potential would result in very accurate values. A similar statement applies to the Joule–Thompson coefficient. The isothermal compressibility was also computed as a derivative from a fit of the volume as a function of the pressure. Within the error limit the results are the same as with the statistical equations. For the thermal pressure and expansion coefficients no experimental values were found.

The speed of sound is typically 1–2% too high, which is slightly more than statistical error. Again the improvement found going from NE1 to NE2 suggests that an improved pair

potential would lead to excellent agreement with experiment.[5] The molar heats at constant volume and at constant pressure are, within statistical error of about 1%, in agreement with the experimental values.

Generally speaking, we expect very accurate derived thermodynamic properties from highly accurate pair potentials without including three-body interactions.

Conclusions

Simulations were performed with two different pair potentials combined with the nonadditive part of the three-body interaction described in the preceding paper. All potentials were obtained from quantum-chemical ab initio calculations. The results showed that three-body interactions have little influence on structure and derived thermodynamic properties, but decrease the pressure and the energy at high densities by a few percent. The important three-body interaction at these high densities is repulsive, that is, not of Axilrod–Teller type. The deviations from experiment of all properties at low temperatures lead us to the conclusion that quantum effects are always important. For the structure this was shown directly by the application of quantum effective potentials,[6] leading to excellent agreement with experiment. The quality of the pair potential plays a crucial role for energy and pressure, has some importance for the derived thermodynamic properties, but is not so critical for the structure.

Here and in the previous work it was shown for the first time that it is possible to simulate a fluid (neon) with chemical accuracy over a wide pressure and temperature range completely ab initio without the use of any empirical parameters. Low temperatures are excluded, since translational quantum effects become important there and cannot be treated adequately in the present classical simulations.

Acknowledgement: This investigation is part of Project 2000-045269.95 supported by the Schweizerischer Nationalfonds zur Förderung der Wissenschaften. We thank the staff of the university computer centre in Basel for their assistance and the Swiss HLR-Rat for a grant of computer time on the national supercomputer.

Received: June 26, 1997 [F739]

[1] D. E. Woon, *Chem. Phys. Lett.* **1993**, *204*, 29–35.
[2] E. Ermakova, J. Solca, H. Huber, M. Welker, *J. Chem. Phys.* **1995**, *102*, 4942–4951.
[3] R. Eggenberger, S. Gerber, H. Huber, D. Searles, *Chem. Phys.* **1991**, *156*, 395–401.
[4] R. Eggenberger, S. Gerber, H. Huber, M. Welker, *Mol. Phys.* **1994**, *82*, 689–699.
[5] R. Eggenberger, H. Huber, M. Welker, *Chem. Phys.* **1994**, *187*, 317–327.
[6] E. Ermakova, J. Solca, H. Huber, D. Marx, *Chem. Phys. Lett.* **1995**, *246*, 204–208.
[7] E. Ermakova, J. Solca, G. Steinebrunner, H. Huber, *Chem. Eur. J.* **1998**, *4*, 377–382.
[8] M. J. Elrod, R. J. Saykally, *Chem. Rev.* **1994**, *94*, 1975–1997.
[9] W. J. Meath, M. Koulis, *J. Mol. Struct. (Theochem)* **1991**, *226*, 1–37.
[10] R. Eggenberger, S. Gerber, H. Huber, D. Searles, M. Welker, *J. Phys. Chem.* **1993**, *97*, 1980–1984.
[11] M. P. Allen, D. J. Tildesley, *Computer Simulation of Liquids*, Clarendon, Oxford, **1987**.
[12] H. Eyring, D. Henderson, W. Jost, *Physical Chemistry*, Academic Press, New York, **1971**.
[13] G. C. Maitland, M. Rigby, E. B. Smith, W. A. Wakeham, *Intermolecular Forces*, Clarendon, Oxford, **1981**.
[14] W. H. Press, B. P. Flannery, S. A. Teukolsky, W. T. Vetterling, *Numerical Recipes (FORTRAN Version)*, Cambridge University Press, Cambridge, **1986**.
[15] F.-M. Tao, *Chem. Phys. Lett.* **1994**, *227*, 401–404.
[16] D. A. McQuarrie, *Statistical Mechanics*, Harper Collins, New York, **1976**.
[17] K. Hermansson, S. Knuts, J. Lindgren, *J. Chem. Phys.* **1991**, *95*, 7486–7496.
[18] R. Eggenberger, S. Gerber, H. Huber, D. Searles, M. Welker, *J. Chem. Phys.* **1992**, *97*, 5898–5904.
[19] R. Eggenberger, S. Gerber, H. Huber, D. Searles, M. Welker, *Mol. Phys.* **1993**, *80*, 1177–1182.
[20] R. Eggenberger, S. Gerber, H. Huber, D. Searles, M. Welker, *J. Comput. Chem.* **1993**, *14*, 1553–1560.
[21] A. Laaksonen, R. E. Wasylishen, *Z. Naturforsch. A* **1995**, *50*, 137–144.
[22] R. Ludwig, F. Weinhold, T. C. Farra, *J. Chem. Phys.* **1995**, *103*, 6941–6950.
[23] D. B. Chesnut, B. E. Rusiloski, *J. Mol. Struct. (Theochem)* **1994**, *314*, 19–30.
[24] V. G. Malkin, O. L. Malkina, G. Steinebrunner, H. Huber, *Chem. Eur. J.* **1996**, *2*, 452–457.
[25] A. Michels, T. Wassenaar, G. J. Wolkers, *Physica* **1965**, *31*, 237–250.
[26] R. Eggenberger, S. Gerber, H. Huber, D. Searles, M. Welker, *J. Chem. Phys.* **1993**, *99*, 9163–9169.

  0947-6539/98/0403-0388 $ 17.50+.50/0